



ELSEVIER

Journal of Chromatography A, 833 (1999) 83–96

JOURNAL OF  
CHROMATOGRAPHY A

## Determination of dissociation constants of $^{99m}\text{Tc}$ Technetium radiopharmaceuticals by capillary electrophoresis

R. Jankowsky\*, M. Friebe, B. Noll, B. Johannsen

*Institut für Bioanorganische und Radiopharmazeutische Chemie, Forschungszentrum Rossendorf e.V., Postfach 510 119, D-01314 Dresden, Germany*

Received 15 April 1998; received in revised form 3 November 1998; accepted 30 November 1998

### Abstract

Capillary electrophoresis was applied to investigate  $\text{p}K_{\text{a}}$  values of  $^{99m}\text{Tc}$  radiotracers used in nuclear medicine. Therefore, the protonation equilibria of the carboxyl groups of  $^{99m}\text{Tc}$ -mercaptoacetylglucylglycylglycine ( $^{99m}\text{Tc}$ -MAG<sub>3</sub>) and  $^{99m}\text{Tc}$ -ethylenecysteine dimer ( $^{99m}\text{Tc}$ -EC) were studied by pH-dependent determination of electrophoretic velocities.  $^{99m}\text{Tc}$ -ethylenecysteine dimer diethyl ester ( $^{99m}\text{Tc}$ -ECD) was used as a non-protonable standard. The capillary electrophoresis system was equipped with a radioactivity detector. Measurements were performed using a pressure-driven capillary zone electrophoresis which allowed runs even in the low pH range. For the determination of  $\text{p}K_{\text{a}}$  values, the electrophoretic velocities of the analytes were referred to the electrophoretic velocities of tetraphenyl ammonium chloride as a positively charged marker. Calculation of  $\text{p}K_{\text{a}}$  values was accomplished by non-linear curve fitting of both structure-based equilibria equations and sigmoidal decay functions to the experimental data.  $^{99m}\text{Tc}$ -MAG<sub>3</sub> was shown to have a carboxyl group  $\text{p}K_{\text{a}}$  value of 4.22. The value for the carboxyl groups of  $^{99m}\text{Tc}$ -EC is 2.90 (determined by structure-based equilibria equations), which represents a common value for both carboxyl groups. By the use of sigmoidal functions, similar values were elucidated. As expected,  $^{99m}\text{Tc}$ -ECD shows no protonation step. © 1999 Elsevier Science B.V. All rights reserved.

**Keywords:** Dissociation constants; Pharmaceutical analysis; Metal complexes; Technetium

### 1. Introduction

Radiotracers based on the radioactive metal nuclide  $^{99m}\text{Tc}$  play an important role in modern nuclear medical diagnosis. They are of widespread use in the visualization of perfusion, tumors or infected tissue [1–8]. The usefulness of these  $^{99m}\text{Tc}$  complex molecules as radiotracers is mainly due to the nearly ideal radiation characteristics and availability of the  $^{99m}\text{Tc}$  nuclide. However, although they are used in daily

clinical routine, little is known about molecular parameters of the radiotracers, since the very low  $^{99m}\text{Tc}$  concentrations in radiopharmaceutical preparations (ca.  $10^{-9}$  M) prevent spectroscopic studies. Alternatively, structural parameters can be identified indirectly. Such parameters are dissociation constants of protonable groups of the tracer molecule. Furthermore, protonation equilibria strongly affect the molecular properties and are thus in part responsible for the pharmacological behaviour of the radiotracer [9]. For these purposes, a reliable method for the determination of dissociation constants is required. A micro-scale determination method is desirable, since

\*Corresponding author. Fax: +49 351 2603232; e-mail: jankow@fz-rossendorf.de

the handled radioactivity amounts have to be as small as possible. Capillary zone electrophoresis (CZE) provides the possibility to elucidate  $pK$  values with small required analyte amounts by the pH-dependent measurement of electrophoretic velocities [10–19]. However, a drawback of the procedure is the sensitivity for changes in the composition of the running electrolytes [20], i.e., electrolytes of very similar properties over the investigated pH range have to be ensured. A further drawback of the capillary electrophoresis method are difficulties in the determination of  $pK_a$  values in the low pH range ( $<4$ ) [13]. Since the required electroosmotic flow (EOF) inside the capillary is very slow at low pH, a conventional CZE is difficult to perform under these conditions [20]. Attempts to overcome this problem suggested the dynamic coating of the capillary by ionic surfactants [13]. However, for the investigation of  $^{99m}\text{Tc}$  radiotracers ionic surfactants cannot be used, because they may cause transchelation effects. Furthermore, the detection of radiotracers based on the  $\gamma$ -emitting nuclide  $^{99m}\text{Tc}$  requires a radioactivity detector. Some applications of capillary electrophoresis with radiodetectors for positron and  $\gamma$ -emitting nuclides have been reported in the past [21–25]. However, drawbacks of the described applications to  $^{99m}\text{Tc}$  complexes are the difficulties in the simultaneous analysis of both cationic and anionic species within the same run [24,25].

In the present work, we describe the coupling of a  $\gamma$ -ray-sensitive radiodetector to a commercially available capillary electrophoresis device. The detection system offers high efficiency through an

improved detector geometry. The detector geometry and its characteristics are described.

Detection of anionic  $^{99m}\text{Tc}$  species in CZE using uncoated capillaries and positive electric fields was realized by the application of a new method. The method bases on an artificially generated flow inside the capillary during runs. This circumvents the problems of CZE at low pH as well as the lack of detectability of anionic  $^{99m}\text{Tc}$  complexes in positive electric fields. By this means, runs at pH of smaller than 1.5 without the addition of surfactants are feasible.

To exclude the influence of the electrolyte composition on the determination of the electrophoretic velocity, analyte velocities were normalized to the velocities of a marker substance (tetraphenyl arsonium cation) with a constant charge of +1 over the pH range.

We applied the detector to the determination of dissociation constants of the radiopharmaceuticals  $^{99m}\text{Tc}$ -mercaptoacetylglycylglycylglycine ( $^{99m}\text{Tc}$ -MAG<sub>3</sub>) and  $^{99m}\text{Tc}$ -ethylenecysteine dimer ( $^{99m}\text{Tc}$ -EC) at the tracer level. As a control,  $^{99m}\text{Tc}$ -ethylenecysteine dimer diethyl ester ( $^{99m}\text{Tc}$ -ECD) was investigated. In Fig. 1, the complex structures are shown.

All investigated complexes contain the  $^{99m}\text{Tc}$  central atom in an oxidation state of +5. In the case of the  $^{99m}\text{Tc}$ -MAG<sub>3</sub> complex, the molecule is anionic when the carboxyl group is protonated. By deprotonation of the carboxyl group, the complex becomes doubly anionic. The  $^{99m}\text{Tc}$ -EC complex is neutral at low pH, and by deprotonation of the

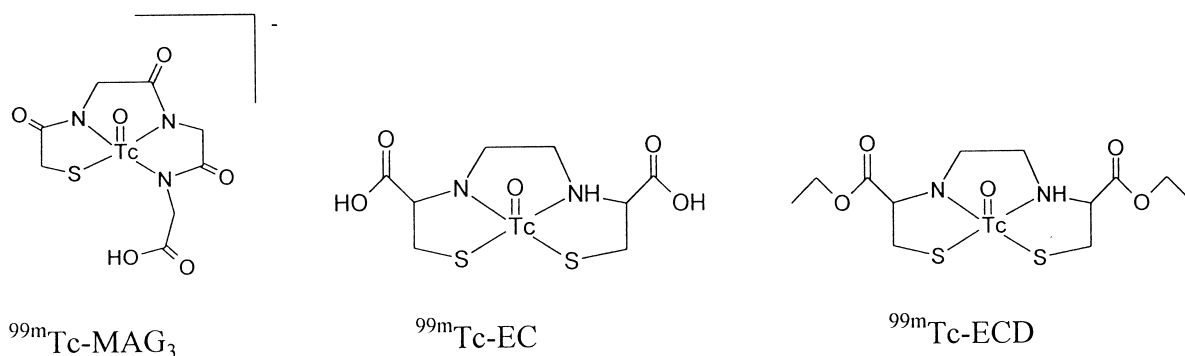


Fig. 1. Complex structures of the investigated  $^{99m}\text{Tc}$  complexes according to Refs. [1–3].

carboxyl groups a double anionic charge is generated.  $pK_a$  values were calculated by fits of theoretical functions derived from the equilibrium constants of the complexes to the experimental velocity data. Furthermore, sigmoidal decay fit functions were employed to elucidate the  $pK_a$  values. For control purposes, the  $^{99m}\text{Tc}$ –ECD complex which should not show a deprotonation step was studied.

## 2. Experimental

### 2.1. CE equipment and radioactivity detector

For measurements, a  $^{3\text{D}}$ CE device (Hewlett-Packard, Waldbronn, Germany) equipped with a diode array detection (DAD) system was used for the investigations. A fused-silica capillary with an inner diameter of 75  $\mu\text{m}$  and an effective length from the capillary inlet to the DAD system of 64 cm was employed. For radioactivity detection, a STEFFI detector with a cylindric NaI(Tl) crystal scintillation probe bearing a circular opening (Raytest, Straubenhardt, Germany) was applied. The detector probe was placed beside the capillary cartridge. Two cylindric lead collimators with conic tips and inner openings of 1.5 mm I.D. were brought into the

crystal opening and placed against each other to yield a slit of 0.5 mm between them. The schematic construction is shown in Fig. 2.

The capillary was lead from the inlet electrode through the detector collimators and further to the DAD and the capillary outlet electrode. The effective length from the capillary inlet to the radioactivity detector was 47.4 cm. Detector signals were processed by a personal computer using an analog-digital converter. The detector cell possessed a volume of 2.2 nl as calculated from capillary inner diameter and the slit between collimators.

### 2.2. Detector tests

Background counting rate of the detector was determined by filling the capillary with electrolyte and counting over several hours. The noise level was elucidated by averaging the obtained counting rate data. Linearity of the detector was checked by filling the capillary with  $\text{Na}^{99m}\text{TcO}_4$  generator eluate and counting over one half-life time of the  $^{99m}\text{Tc}$  nuclide (6 h) to monitor the radioactive decay. The obtained detector data were computed into their natural logarithm and plotted against decay time.

To test detector efficiency, a solution of  $\text{Na}^{99m}\text{TcO}_4$  (30  $\mu\text{l}$ ) was measured by an external

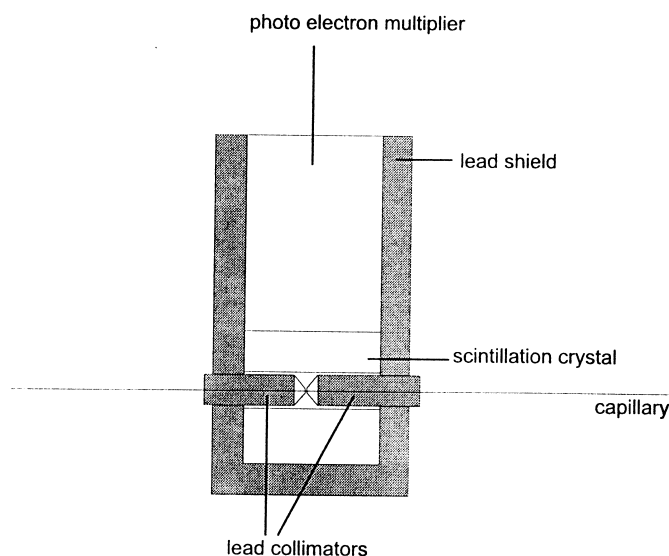


Fig. 2. Schematic construction of the radioactivity detector.

NaI scintillation measuring device. Subsequently, the capillary was filled with that eluate and the detector response was registered. The counts measured by the radioactivity detector were corrected for detector cell volume. Measurements were repeated four times.

### 2.3. $^{99m}\text{Tc}$ complexes sample preparation

$^{99m}\text{Tc}$ -MAG<sub>3</sub> in kit form was a kind gift from ROTOP Nuclear Engineering and Analytics (Dresden, Germany). The  $^{99m}\text{Tc}$ -EC kit was provided by the Department of Radiopharmaceuticals Production (Medical University Foundation, Lodz, Poland). Kits were prepared with Na<sup>99m</sup>TcO<sub>4</sub> in saline obtained from a Ultra-Technekow generator (Mallinckrodt Medical, Petten, The Netherlands).  $^{99m}\text{Tc}$ -ECD (DuPont, Bad Homburg, Germany) was a gift from the Clinic for Nuclear Medicine at the University Hospital of the Dresden University of Technology, (Dresden, Germany). All radiopharmaceutical preparations contained radioactivity amounts of ca. 200 MBq/ml. For pK<sub>a</sub> determinations, the  $^{99m}\text{Tc}$  complex solutions were spiked with acetone as a neutral marker. Additionally, small amounts of tetraphenyl arsonium chloride (AsPPh<sub>4</sub><sup>+</sup>Cl<sup>-</sup>) were added to the sample solutions which served as a marker with a single positive charge. To ensure its inertness over the pH range, the absence of protonation steps at the internal cationic reference was checked by conventional titration using a Mettler DL67 Titrator (Mettler-Toledo, Giessen, Germany).

### 2.4. CE electrolytes

Running electrolytes were prepared by adding 0.01 M HCl/0.01 M NaOH to a 0.01 M solution of citric acid in 0.02 M NaOH. pH values were measured using a Delta 320 device (Mettler-Toledo, Giessen, Germany). Electrolyte ionic strengths were calculated as described [10]. The electrolytes used for the measurements are listed in Table 1.

### 2.5. CE run conditions

Prior to each run, the capillary was rinsed with electrolyte for 2 min. Injection was done hydrodynamically (analyte, 50 mbar/3 s; electrolyte, 50 mbar/1 s). During runs, voltages of +25 kV were

Table 1  
CE running electrolytes used for pK<sub>a</sub> determination

$^{99m}\text{Tc}$ complex	pH	Ionic strength (M)	
$^{99m}\text{Tc}$ -MAG <sub>3</sub>	2.71	0.034	
	3.34	0.039	
	3.82	0.044	
	4.27	0.052	
	4.53	0.059	
	5.08	0.072	
	5.59	0.075	
	6.05	0.049	
	$^{99m}\text{Tc}$ -EC	1.3	0.02
		1.9	0.03
2.4		0.033	
2.7		0.034	
3.4		0.04	
3.7		0.042	
4.3		0.052	
4.8		0.067	
$^{99m}\text{Tc}$ -ECD	5.3	0.062	
	1.5	0.024	
	2.7	0.034	
	3.3	0.039	
	3.9	0.044	
	4.3	0.052	
	4.6	0.59	
	5.1	0.068	
	5.6	0.055	
	6.0	0.049	
	6.6	0.046	

applied, thus the electroosmotic flow was directed towards the outlet electrode (cathode). To ensure a sufficient flow inside the capillary over the entire pH range, an external air pressure of 50 mbar was applied onto the capillary inlet vial during runs [27]. This pressure was realized by the built-in air pump of the CE device. Detections of the marker substances were carried out at 214 nm (AsPPh<sub>4</sub><sup>+</sup>) and 254 nm (acetone).

### 2.6. Validation of the pressure-driven CZE

To check the constancy of the applied pressure during runs, five runs of the  $^{99m}\text{Tc}$ -EC complex with an electrolyte pH of 2.4 were performed. The detection times of the complex at the radioactivity detector were recorded and compared in view of their reproducibility.

### 2.7. Determination of $pK_a$ values

Determinations of  $pK_a$  values of the  $^{99m}\text{Tc-MAG}_3$  complex and the  $^{99m}\text{Tc-EC}$  complex were performed using the computer program Origin 4.1 (Microcal, Northampton, MA, USA) by non-linear fits to Eqs. (13) and (17), respectively (see Section 3). For sigmoidal decay function fits, a Boltzmann-like sigmoidal decay function of the general form

$$y = \frac{A_1 - A_2}{1 + e^{(x-x_0)/dx}} + A_2$$

was modified with the parameters of the electrophoretic velocity curves (see Section 4).

### 3. Theory

The electrophoretic mobilities of the complexes are proportional to their migration velocities [10,13–18]. In order to circumvent electrolyte effects on the velocities of the complexes, their electrophoretic velocities were normalized to the velocity of the  $\text{AsPPh}_4^+$  cation marker as internal reference which was measured simultaneously in each run. The velocities of the compounds in the complex solutions were determined by

$$v_{+1} = \frac{L_{\text{DAD}}}{t_{+1}}, \quad (1)$$

$$v_0 = \frac{L_{\text{DAD}}}{t_0} \quad (2)$$

and

$$v_{\text{C}} = \frac{L_{\text{Act}}}{t_{\text{C}}} \quad (3)$$

where  $v_{+1}$  is the velocity of the internal reference;  $v_0$  is the velocity of the neutral marker;  $v_{\text{C}}$  is the velocity of the  $^{99m}\text{Tc}$  complex;  $L_{\text{DAD}}$  is the effective length from the capillary inlet to the diode array detector (64 cm);  $L_{\text{Act}}$  is the effective length from the capillary inlet to the radioactivity detector (47.4 cm);  $t_{+1}$  is the migration time of the internal reference;  $t_0$  is the migration time of the neutral marker; and  $t_{\text{C}}$  is the migration time of the  $^{99m}\text{Tc}$  complex.

The velocities of both the internal reference and the analyte consist of contributions of their electro-

phoretic velocity and the flow inside the capillary. The contribution of the latter was rejected by

$$v_{+1,E} = v_{+1} - v_0 \quad (4)$$

and

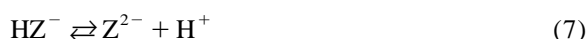
$$v_{\text{C,E}} = v_{\text{C}} - v_0 \quad (5)$$

where  $v_{+1,E}$  is velocity of the internal reference due to its electrophoretic mobility; and  $v_{\text{C,E}}$  is the velocity of the  $^{99m}\text{Tc}$  complex due to its electrophoretic mobility, since the velocity of the neutral marker is only determined by the flow inside the capillary. The relative electrophoretic velocity of the  $^{99m}\text{Tc}$  complex versus the internal reference ( $v_{\text{rel}}$ ) was then calculated by

$$v_{\text{rel}} = \frac{v_{\text{C,E}}}{v_{+1,E}} \quad (6)$$

Hence, negative values for  $v_{\text{rel}}$  indicate anionic complexes.

The  $^{99m}\text{Tc-MAG}_3$  complex bears a single negative net charge at low pH when the carboxyl group is protonated (see Fig. 1). Thus, the equilibrium



with the thermodynamical equilibrium constant

$$K_a = \frac{\gamma_{\text{H}^+} \gamma_{\text{Z}^{2-}} [\text{H}^+] [\text{Z}^{2-}]}{\gamma_{\text{HZ}^-} [\text{HZ}^-]} \quad (8)$$

where  $\gamma_{\text{H}^+}$  is the activity coefficient of the protons;  $\gamma_{\text{Z}^{2-}}$  is the activity coefficient of the deprotonated complex; and  $\gamma_{\text{HZ}^-}$  is the activity coefficient of the protonated complex can be formulated. The activity coefficients of both the protonated and the deprotonated complexes can be determined by

$$-\log \gamma_{\text{Z}^{2-}} = \frac{0.5085 \times 4 \times \sqrt{I}}{1 + 0.3281 \times 10 \times \sqrt{I}}$$

and

$$-\log \gamma_{\text{HZ}^-} = \frac{0.5085 \times 1 \times \sqrt{I}}{1 + 0.3281 \times 10 \times \sqrt{I}} \quad (9)$$

where  $I$  is the ionic strength of the electrolyte. The hydrated diameter for the complex is assumed to be 10 Å [10,26].

Hence, the relationship

$$\frac{-\log \gamma_{Z^{2-}}}{-\log \gamma_{HZ^-}} = 4 \quad (10)$$

can be derived.

Substitution of  $\gamma_{Z^{2-}}$  in Eq. (8) gives

$$K_a = \frac{\gamma_{H^+} \gamma_{HZ^-}^3 [H^+] [Z^{2-}]}{[HZ^-]} \quad (11)$$

The ratio  $[Z^{2-}]/[HZ^-]$  can be expressed in terms of the protonation grade  $\alpha$  of the carboxyl group. Since the deprotonation is connected with a change in the electrophoretic mobility of the complex, the measurable electrophoretic velocities may be used to elucidate the  $[Z^{2-}]/[HZ^-]$  ratio as described in Ref. [10]. However, the complex with a protonated carboxyl group bears a single negative charge, thus its electrophoretic velocity does not equal zero and has to be considered in the calculation. The following equation may be derived:

$$\frac{[Z^{2-}]}{[HZ^-]} = \frac{\alpha}{1 - \alpha} = \frac{v_{rel,C} - v_{rel,HZ^-}}{v_{rel,Z^{2-}} - (v_{rel,C} - v_{rel,HZ^-})} \quad (12)$$

where  $\alpha$  is the protonation grade of the carboxyl group;  $v_{rel,C}$  is the measured relative velocity of the complex versus the cationic internal reference (see Eq. (6));  $v_{rel,HZ^-}$  is the relative velocity of the fully protonated complex; and  $v_{rel,Z^{2-}}$  is the relative velocity of the fully deprotonated complex minus the velocity of the protonated complex.

Substitution and transformation of Eq. (11) gives

$$v_{rel,C} - \frac{v_{rel,Z^{2-}} K_a}{\gamma_{HZ^-}^3 \gamma_{H^+} [H^+] + K_a} + v_{rel,HZ^-} \quad (13)$$

where the proton activity  $\gamma_{H^+} [H^+]$  can be calculated from the measured pH. Determination of  $K_a$  and velocity of the fully protonated complex can be carried out by non-linear curve fitting of  $v_{rel,C}/\gamma_{HZ^-}^3 \gamma_{H^+} [H^+]$  data pairs to Eq. (13).

The  $^{99m}\text{Tc}$ -EC complex is neutral when both carboxyl groups are protonated (see Fig. 1). By increasing the electrolyte pH, the carboxyl groups deprotonate and generate two negative charges at the complex. Due to their chemical similarity, it can be assumed that the two carboxyl groups deprotonate simultaneously, i.e., their  $pK_a$  values are equal. For

simplification, the deprotonation of each carboxyl group can be considered as



However, in the complex the  $\text{HZ}^-$  ion is not really existent, since the simultaneous deprotonation of both carboxyl groups leads to the occurrence of the doubly negatively charged complex ion  $\text{Z}^{2-}$ . Thus, the amount of  $\text{HZ}^-$  is equal to the amount of  $\text{Z}^{2-}$ . For the calculation of the thermodynamical equilibrium constant of equilibrium (Eq. (14)), the activity coefficient of the really existing  $\text{Z}^{2-}$  complex ion has to be used. Therefore,  $K_a$  can be expressed by

$$K_a = \frac{\gamma_{H^+} \gamma_{Z^{2-}} [H^+] [HZ^-]}{[\text{H}_2\text{Z}]} \quad (15)$$

where  $\gamma_{H^+}$  is the proton activity coefficient; and  $\gamma_{Z^{2-}}$  is the activity coefficient of the fully deprotonated complex.

The activity coefficient of the fully protonated, neutral complex  $\text{H}_2\text{Z}$  is assumed to be 1, the activity coefficient of the fully deprotonated complex can be calculated by

$$-\log \gamma_{Z^{2-}} = \frac{0.5085 \times 4 \times \sqrt{I}}{1 + 0.3281 \times 10 \times \sqrt{I}}$$

where  $I$  is the ionic strength of the electrolyte and the hydrated diameter of the complex is assumed to be  $10 \text{ \AA}$  [10,26].

Similarly to Eq. (12), the ratio  $[HZ^-]/[\text{H}_2\text{Z}]$  can be expressed by the protonation grade of the carboxyl groups and the electrophoretic velocity of the complex. The electrophoretic velocity of the complex is solely caused by deprotonated carboxyl groups, where each contributes exactly the half to the total electrophoretic velocity of the complex. Hence, it can be written

$$\frac{[HZ^-]}{[\text{H}_2\text{Z}]} = \frac{\alpha}{1 - \alpha} = \frac{\frac{v_{rel,C}}{2}}{v_{rel,HZ^-} - \frac{v_{rel,C}}{2}} \quad (16)$$

where  $\alpha$  is the protonation grade of the carboxyl groups;  $v_{rel,C}$  is the measured relative velocity of the complex versus the cationic internal reference (see Eq. (6)); and  $v_{rel,HZ^-}$  is the relative velocity of the deprotonated  $\text{HZ}^-$  complex ion.

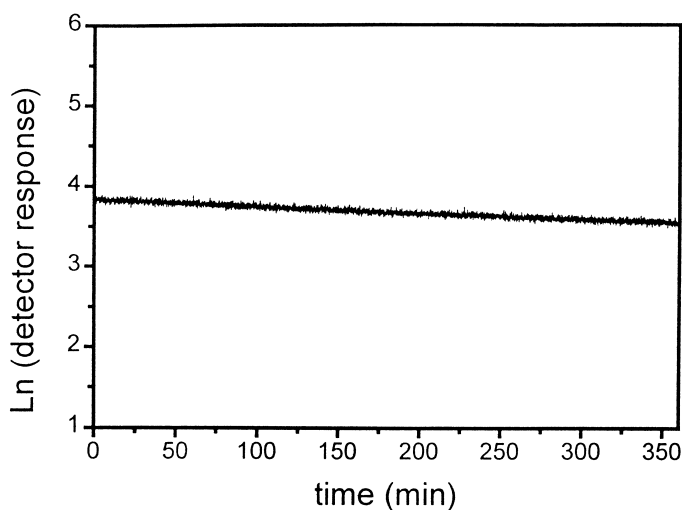


Fig. 3. Detector linearity plot.

Substitution in Eq. (16) yields

$$v_{\text{rel,C}} = 2 \times \frac{v_{\text{rel,HZ}} - K_a}{\gamma_{\text{Z}^2} - \gamma_{\text{H}^+} [\text{H}^+] + K_a} \quad (17)$$

Data pairs of  $v_{\text{rel,C}}$  and  $\gamma_{\text{Z}^2} - \gamma_{\text{H}^+} [\text{H}^+]$  can be processed as described for the  $^{99\text{m}}\text{Tc-MAG}_3$  complex.

## 4. Results and discussion

### 4.1. Detector characteristics

A linearity test was performed by filling the capillary with  $\text{Na}^{99\text{m}}\text{TcO}_4$  generator eluate (650 MBq/ml) and recording the detector response over 6

h. The  $\gamma$ -detector showed a linear response. In Fig. 3, the logarithmic plot of the detector signals versus the  $^{99\text{m}}\text{Tc}$  decay time is shown.

To check the linearity, a linear curve fit was performed and yielded a regression coefficient of 0.92. Thus, linearity of the detector response in the range up to 150 cps can be assumed. The background noise level of the detector was determined by filling the capillary with electrolyte and recording the detector response over several hours. An averaged detector signal of 3.2 cps was obtained. As calculated from capillary inner diameter and the slit between the lead collimators of the radioactivity detector, the detector cell volume was 2.2 nl. The detector efficiency test yielded data as shown in Table 2.

Table 2  
Detector efficiency test

Measurement number	Radioactivity measured by external scintillation device (30 $\mu\text{l}$ )	Radioactivity measured by CE detector (2.2 nl)	Detector efficiency <sup>a</sup> (%)
1	$2.756 \times 10^6$ cps	173.5 cps	85.5
2	$2.813 \times 10^6$ cps	176.5 cps	85.2
3	$2.721 \times 10^6$ cps	176.0 cps	87.9
4	$2.780 \times 10^6$ cps	170.0 cps	83.1

<sup>a</sup>In order to correct for different measured detector cell volumes, the radioactivity amount measured by the CE detector was multiplied by the ratio of the measured volumes in the external device (30  $\mu\text{l}$ ) and in the CE detector cell (2.2 nl). The detector efficiency was determined by comparing the corrected CE detector data to the data from the external device.

A mean efficiency of 85.4% could be obtained. This relatively high value is mainly due to the detector geometry which allows the detection of emitted  $\gamma$ -rays around the capillary. The small detector cell volume can be considered as a further advantage. Thus, a high resolution is possible, although the sensitivity is worse if small detector cell volumes are used. However, for radiopharmaceutical purposes dealing with much higher radioactivity amounts than this study, the sensitivity should be sufficient.

#### 4.2. Pressure-driven CZE

The detectability of fast anionic complexes and possibly cationic substances represents a problem in conventional CZE. Since the electrophoretic velocity as well as the EOF are proportional to the applied electric field, the flow inside the capillary has to be artificially increased to detect both cationic and fast anionic substances within one run when a positive electric field is used. Therefore, an external air pressure of 50 mbar was applied onto the capillary inlet vial. By this means, the flow inside the capillary was increased and a detection of all analyte species became possible. To check the constancy of the applied pressure, five runs of  $^{99m}\text{Tc-EC}$  at an electrolyte pH of 2.4 were performed. The obtained migration times varied between 3.58 and 3.64 min. However, an additional flow inside the capillary will alter the CZE-typical flow profile. Thus, a slight peak broadening was observed at low pH. At higher pH, the peak broadening effects were negligible.

#### 4.3. Determination of $pK_a$ values

Pressure-driven CZE was used to determine the acidity constants of  $^{99m}\text{Tc-MAG}_3$  and  $^{99m}\text{Tc-EC}$ . Therefore, the relative electrophoretic velocities of the  $^{99m}\text{Tc}$  complexes referring to a positively charged internal standard were recorded in dependence of the electrolyte pH. The positively charged cation  $\text{AsPPh}_4^+$  was used as a cationic standard. Acetone served as neutral marker. Prior to the measurements, the cationic reference was titrated by an acid–base titration and showed no protonation step in the area from pH 1 to 12.5 showing that it can be considered as inert. Attempts to record pH

curves without the internal cationic reference resulted in curves of very poor quality, i.e., data points scattered significantly.

CE runs of the radiopharmaceutical preparations were monitored at three channels. The first channel, the radioactivity detection, delivered the migration time of the  $^{99m}\text{Tc}$  complexes. The second channel, DAD at 214 nm showed the migration time of the cationic reference and the third channel, DAD at 254 nm indicated the detection time of acetone. The obtained signal pattern for a run of  $^{99m}\text{Tc-EC}$  is shown in Fig. 4.

For  $^{99m}\text{Tc-MAG}_3$ , the pH curve as depicted in Fig. 5 was obtained. In the figure, the pH value was corrected for the activity coefficients of the complex ( $\text{pH}_C$ ) by

$$\text{pH}_C = \text{pH} - 3 \log \gamma_{\text{HZ}^-} \quad (18)$$

as derived from Eq. (13). In Fig. 6, the relative velocity of the  $^{99m}\text{Tc}$  complex is plotted versus with the proton activity which was corrected correspondingly to  $\text{pH}_C$ .

By a non-linear curve fit of Eq. (13), the fit parameters presented in Table 3 were obtained.

A  $pK_a$  value of 4.22 for the glycyl carboxyl group was elucidated, which is significantly higher than the value of 2.35 for the free glycine amino acid [28]. This is attributed to the absence of any free amino group in the vicinity of the carboxyl group which could serve as proton acceptor. Furthermore, the detection of the carboxyl group represents a hint to the structural identity of the  $^{99m}\text{Tc-MAG}_3$  complex at the tracer level (see Fig. 1). This is further supported by the fit of the theoretical function to the experimental data. The complex bears a single negative charge at low pH, while the deprotonation of the carboxyl group leads to a double negative charge.

For the  $^{99m}\text{Tc-EC}$  complex, the curves presented in Figs. 7 and 8 were obtained. The measured pH was corrected ( $\text{pH}_C$ ) for the activity coefficient of the doubly charged complex anion by

$$\text{pH}_C = \text{pH} - \log \gamma_{\text{Z}^{2-}} \quad (19)$$

Correction of the proton activity was performed according to Eq. (19).

A non-linear curve fit of Eq. (17) to the ex-



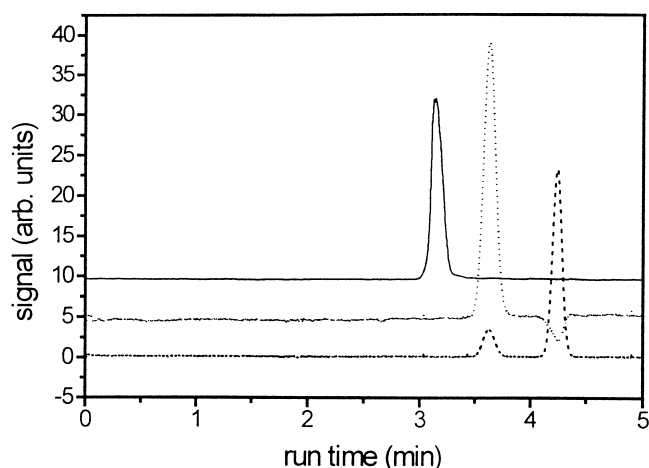


Fig. 4. Signal pattern for a run of  $^{99m}\text{Tc-EC}$ ; solid line, radioactivity detection; dotted line, DAD at 214 nm; dashed line, DAD at 254 nm; electrolyte, citric acid-HCl, pH 1.9; voltage, +25 kV; current, 45  $\mu\text{A}$ , 50 mbar pressure onto the capillary inlet vial during run.

perimental data yielded fit parameters given in Table 3. A  $\text{p}K_{\text{a}}$  value of 2.90 was determined for the carboxyl groups. The value is significantly higher than 1.9 for the free cysteine ligand [28]. This can be explained by the chemical modification of the cysteine as well as by the coordination of the metal atom. A relative complex velocity difference of  $-0.69$  was elucidated for the deprotonation of each carboxyl group, which is much smaller than the velocity difference of the protonated/deprotonated

$^{99m}\text{Tc-MAG}_3$  complex. This is due to the increased hydrated diameter of the  $^{99m}\text{Tc-EC}$  complex which is inversely proportional to its electrophoretic velocity. The obtained absolute charges of the  $^{99m}\text{Tc-EC}$  complex are coherent with the complex structure (Fig. 1). At low pH, the carboxyl groups are protonated, thus the complex is neutral. By increasing the pH, the carboxyl groups deprotonate and lead to a double negative charge of the complex. The assumption of chemically equivalent carboxyl

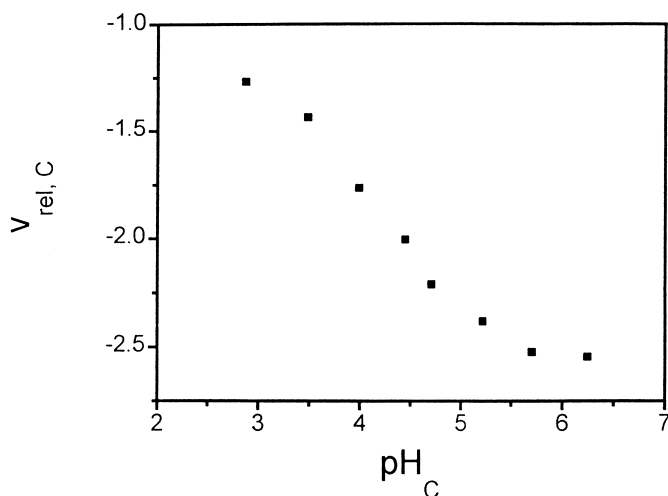


Fig. 5. Relative velocity versus  $\text{pH}_{\text{C}}$  curve of the  $^{99m}\text{Tc-MAG}_3$  complex. The corrected pH values ( $\text{pH}_{\text{C}}$ ) were calculated by Eq. (18).

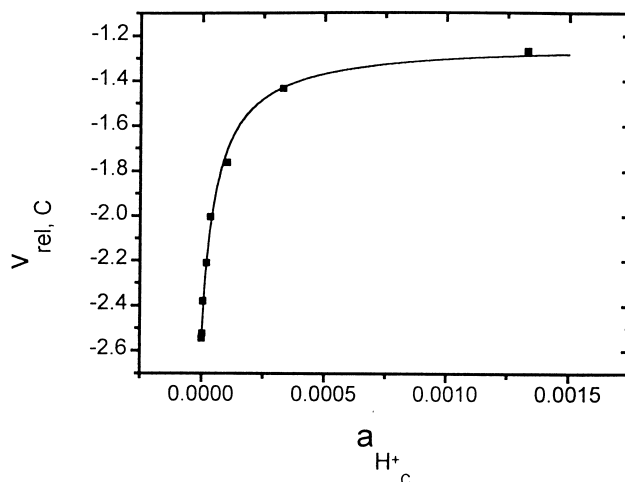


Fig. 6. Relative velocity versus proton activity curve of the  $^{99m}\text{Tc-MAG}_3$  complex solid line: fit to Eq. (13). The corrected proton activities  $a_{\text{H}^+_{\text{C}}}$  were calculated corresponding to Eq. (18).

Table 3

Fit parameters for non-linear curve fits of  $^{99m}\text{Tc-MAG}_3$  and  $^{99m}\text{Tc-EC}$

Complex	Fit parameter	Value
$^{99m}\text{Tc-MAG}_3$	$K_a$	$6 \times 10^{-5} M$
	$v_{\text{rel,HZ}^-}$	-1.23
	$v_{\text{rel,Z}^{2-}}$	-1.31
	$\text{p}K_a$	4.22
$^{99m}\text{Tc-EC}$	$K_a$	0.00127 M
	$v_{\text{rel,HZ}^-}$	-0.69
	$\text{p}K_a$	2.90

groups could be confirmed, since only a single protonation step is detectable.

For  $^{99m}\text{Tc-ECD}$ , the pH curve as shown in Fig. 9 was recorded.

No protonation step can be detected, thus the neutral complex does not possess protonable groups in the investigated pH range. This is in accordance to the esterificated carboxyl groups in the complex.

However, the shown  $\text{p}K_a$  determinations are fea-

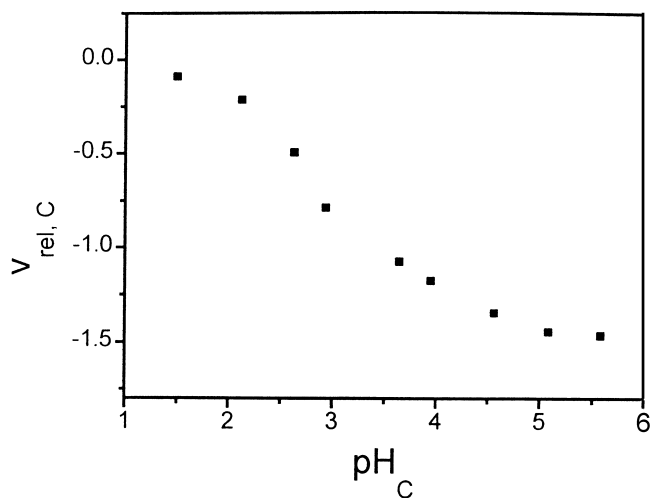


Fig. 7. Relative velocity versus  $\text{pH}_{\text{C}}$  curve of the  $^{99m}\text{Tc-EC}$  complex. The corrected pH values ( $\text{pH}_{\text{C}}$ ) were calculated by Eq. (19).

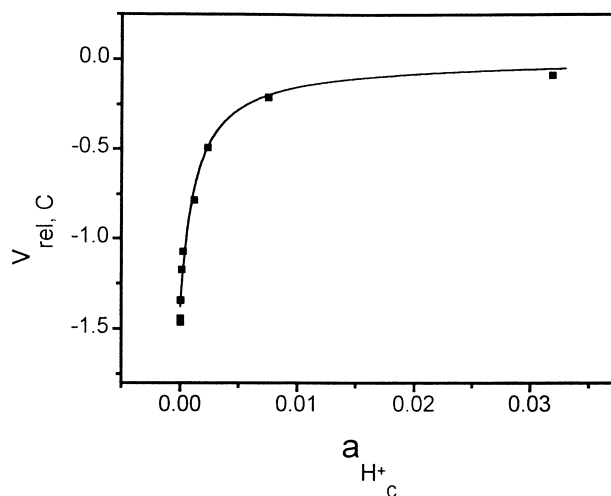


Fig. 8. Relative velocity versus proton activity curve of the  $^{99m}\text{Tc}$ -EC complex solid line: fit to Eq. (17). The corrected proton activities  $a_{\text{H}^+}$  were calculated corresponding to Eq. (19).

ible only if the complex structures are known. If the structures of the  $^{99m}\text{Tc}$  complexes are completely unknown, no accurate determinations can be performed by this means. Instead of this,  $\text{p}K_a$  values have to be elucidated using the fact that the dissociation constants equal the half-height pH of the velocity–pH curve of the complex. Therefore, the

experimental data points can be fitted with a sigmoidal decay using a Boltzmann model:

$$v_{\text{rel,C}} = \frac{v_{\text{rel,HZ}^-} - v_{\text{rel,Z}^-}}{1 + e^{\frac{\text{pH}}{d(\text{pH})}}} + v_{\text{rel,Z}^-} \quad (20)$$

where  $v_{\text{rel,C}}$  is the measured relative velocity of the

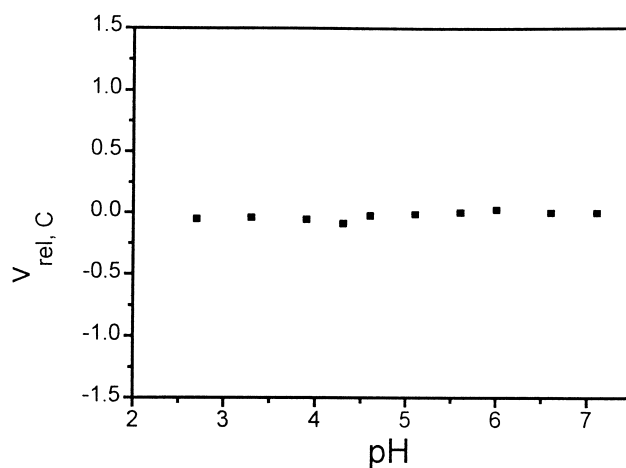


Fig. 9. Relative velocity versus pH curve of the  $^{99m}\text{Tc}$ -ECD complex.

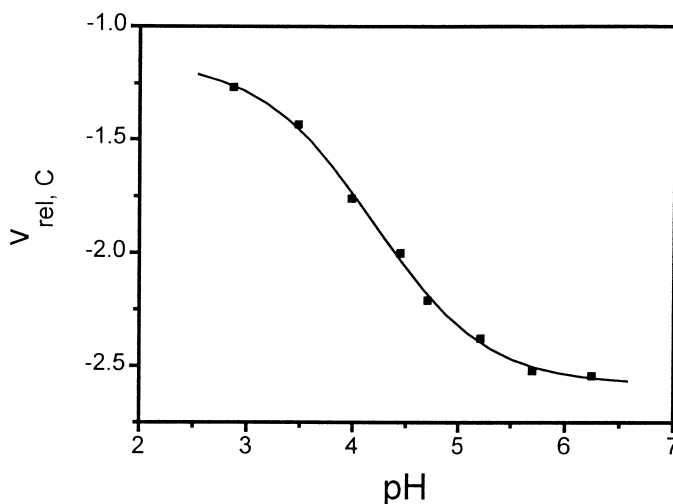


Fig. 10. Velocity–pH<sub>c</sub> curve of <sup>99m</sup>Tc–MAG<sub>3</sub> solid line, sigmoidal fit of Eq. (20).

complex;  $v_{\text{rel,HZ}^-}$  is the relative velocity of the protonated complex;  $v_{\text{rel,Z}^-}$  is the relative velocity of the deprotonated complex; and  $d(\text{pH})$  is the step width.

The half-height pH of the fitted function represents the  $\text{p}K_{\text{a}}$  value. Using this model, the velocity–pH curves of <sup>99m</sup>Tc–MAG<sub>3</sub> and <sup>99m</sup>Tc–EC were analyzed. The curves with their sigmoidal fits are shown in Figs. 10 and 11.

The fit parameters are given in Table 4.

The obtained  $\text{p}K_{\text{a}}$  values are nearly exactly identical to the values determined by non-linear curve

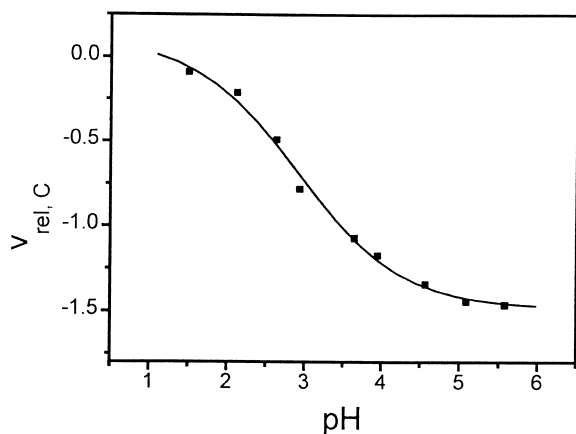


Fig. 11. Velocity–pH<sub>c</sub> curve of <sup>99m</sup>Tc–EC solid line, sigmoidal fit of Eq. (20).

fittings of the theoretical equations. Velocity values of the protonated/deprotonated complexes also correlate with the non-linear curve fits. It is worth mentioning that the fit parameters  $v_{\text{HZ}^-}$  and  $v_{\text{Z}^-}$  represent the absolute velocities of the protonated and deprotonated species, respectively, regardless of the absolute charges of the protonated species.

## 5. Conclusions

In the present study, capillary electrophoresis coupled with a radioactivity detection system was used to determine  $\text{p}K_{\text{a}}$  values of <sup>99m</sup>Tc radiopharmaceuticals. The study shows the applicability to <sup>99m</sup>Tc radiopharmaceutical preparations. The con-

Table 4  
Fit parameters of the sigmoidal fits to the experimental data of <sup>99m</sup>Tc–MAG<sub>3</sub> and <sup>99m</sup>Tc–EC

Complex	Fit parameter	Value
<sup>99m</sup> Tc–MAG <sub>3</sub>	$v_{\text{rel,HZ}^-}$	–1.14
	$v_{\text{rel,Z}^-}$	–2.58
	$d(\text{pH})$	0.54
	$\text{p}K_{\text{a}}$	4.18
<sup>99m</sup> Tc–EC	$v_{\text{rel,HZ}^-}$	0.118
	$v_{\text{rel,Z}^-}$	–1.48
	$d(\text{pH})$	0.67
	$\text{p}K_{\text{a}}$	2.90

structed radioactivity detector is characterized by a high efficiency realized by an improved detector geometry. In the investigated radioactivity range, the detector shows a linear behaviour as well as a low background noise. A high resolution is provided by a small measuring cell. Its cell volume of 2.2 nl is comparable to UV detector cell volumes in capillary electrophoresis. However, the small detector cell is connected with a loss in detector sensitivity. As a future improvement, the sensitivity will be increased by the use of an extension in the capillary inner diameter (bubble cell) within the detector cell as used for UV detection.

The pressure-driven capillary electrophoresis offers the possibility to detect both cations as well as highly mobile metal anions within one run. The principle should be easily transferable to other systems. However, a reliable pressure is required for the method. Since most CE devices use built-in air pressure pumps, the procedure should be feasible by most commercially available devices. Although the flow inside the capillary is altered by the application of an external pressure, no significant peak broadening was observed. Obviously, the typical flow profile remains widely, so that the CE-typical separation sharpness can be ensured. By this means, separation runs at very low pH are possible without the use of electrolyte additives. The latter is very advantageous in the analysis of metal-containing systems, since electrolyte additives represent possible metal chelators and may thus change the molecular structures of the analytes during runs. The detection of fast anions besides cationic complexes within one run is especially useful in the quality control of  $^{99m}\text{Tc}$  radiopharmaceuticals in clinical routine, since all preparations have to be checked for residues of non-reacted  $\text{Na}^{99m}\text{TcO}_4$  generator eluate. Furthermore, the analysis times are decreased significantly.

For p*K* determination, the use of a cationic internal reference was shown to be very useful. Only poor curves were obtained if the analyte velocities were not referred to the values of the internal standard. By the use of an internal reference, the electrolyte composition as a run parameter can be excluded, since the electrolyte parameters equally influence the velocities of both the reference and the analyte. The applied  $\text{AsPPh}_4^+$  reference is very suitable, since its charge remains constantly over the

pH range and it delivers a sufficient UV absorption due to its aromatic ring systems.

Since the charge relationships are much more complicated in the case of  $^{99m}\text{Tc}$  complexes compared to simple organic acids or bases, every complex has to be considered separately in view of its theoretical dependence of the electrophoretic velocity on the pH. Therefore, the coherence between the deprotonation grade and the electrophoretic velocity has to be adapted to the absolute charges of both the protonated and deprotonated complex species. Special attention has to be drawn to the careful consideration of activity coefficients. The obtained theory curve fit to the experimental data represents a useful control of the complex structure, since reasonable fit parameters can only be obtained if the structure model for the complex is accurate. Alternatively, p*K* data can be obtained by sigmoidal curve fits to the pH–velocity curves. This was shown to deliver accurate parameters.

In the case of the  $^{99m}\text{Tc}$ –MAG<sub>3</sub> complex, the determined p*K* value of 4.2 corresponds to the expected value for the carboxyl group. The value for the  $^{99m}\text{Tc}$ –EC complex is significantly lower, which is due to the different complex structure and metal coordination sphere. Considering the  $^{99m}\text{Tc}$ –ECD complex, no protonation step was detectable and thus no protonable groups are existent. For all complexes, the complex structures could be confirmed, representing a step towards the better understanding of the molecular structures of complexes at the very low concentrated  $^{99m}\text{Tc}$  tracer level.

In the future, the determination of p*K* values will be extended to other  $^{99m}\text{Tc}$  complex classes which represent potential radiotracers. Such complexes, e.g., mixed-ligand systems, often contain protonable nitrogen atoms and are, therefore, well suited to determine their p*K* values by CE means.

## References

- [1] W.A. Volkert, S. Jurisson, Topics Curr. Chem. 176 (1996) 123.
- [2] B. Johannsen, H. Spies, Topics Curr. Chem. 176 (1996) 77.
- [3] S. Jurisson, D. Berning, W. Jia, D. Ma, Chem. Rev. 93 (1993) 1137.
- [4] E. Deutsch, K. Libson, S. Jurisson, L.F. Lindoy, Progr. Inorg. Chem. 30 (1983) 75.

- [5] M.J. Clarke, L. Podbielski, *Coord. Chem. Rev.* 77 (1987) 275.
- [6] A.M. Verbruggen, *Eur. J. Nucl. Med.* 17 (1990) 346.
- [7] E.C. Constable, C.E. Housecroft, *Coord. Chem. Rev.* 131 (1994) 153.
- [8] W.C. Eckelman, *Eur. J. Nucl. Med.* 22 (1995) 249.
- [9] B. Johannsen, H. Spies, *Trans. Met. Chem.* 22 (1997) 218.
- [10] J.A. Cleveland Jr., M.H. Benkő, S.J. Gluck, Y. M Walbroehl, *J. Chromatogr. A* 652 (1993) 301.
- [11] L.Z. Benet, J.E. Goyan, *J. Pharm. Sci.* 56 (1967) 665.
- [12] A. Roda, A. Minutello, A. Fini, *J. Lipid Res.* 31 (1990) 1433.
- [13] S.J. Gluck, K.P. Steele, M.H. Benkő, *J. Chromatogr. A* 745 (1996) 117–125.
- [14] J.M. Beckers, F.M. Everaerts, M.T. Ackermans, *J. Chromatogr.* 537 (1991) 407.
- [15] J. Cai, J.T. Smith, Z. E Rassi, *J. High Resolut. Chromatogr.* 15 (1992) 30.
- [16] S.J. Gluck, J.A. Cleveland, *J. Chromatogr. A* 680 (1994) 43.
- [17] S.J. Gluck, J.A. Cleveland, *J. Chromatogr. A* 680 (1994) 49.
- [18] J.A. Cleveland, C.L. Martin, S.J. Gluck, *J. Chromatogr. A* 679 (1994) 167.
- [19] Y. Ishihama, Y. Oda, N. Asakawa, *J. Pharm. Sci.* 83 (1994) 1500.
- [20] H. Engelhardt, W. Beck, T. Schmidt, *Kapillarelektrophorese—Methoden und Möglichkeiten*, Vieweg, Braunschweig, Wiesbaden, 1994.
- [21] G. Westerberg, B. Langstrom, *Appl. Rad. Isot.* 45 (1994) 773.
- [22] G. Westerberg, H. Lundqvist, F. Kilar, B. Langstrom, *J. Chromatogr.* 645 (1993) 319.
- [23] D. Kaniansky, P. Havasi, *Trends Anal. Chem.* 2 (1983) 197.
- [24] K.D. Altria, C.F. Simpson, A.K. Bharij, A.E. Theobald, *Electrophoresis* 11 (1990) 732.
- [25] G.C. Krijger, H.A. Claessens, H.T. Wolterbeek, *Chem. Spec. Bioavail.* 8 (1996) 29.
- [26] J. Kielland, *J. Am. Chem. Soc.* 59 (1937) 1675.
- [27] R. Jankowsky, M. Friebe, *German Patent Appl.*, 197 50 832.4 (1998).
- [28] D.R. Lide (Ed.), *CRC Handbook of Chemistry and Physics*, 73rd ed., CRC Press, Boca, Raton, FL, 1993.